

Synthesis and Biological Evaluation of RGD and *iso*DGR–Monomethyl Auristatin Conjugates Targeting Integrin $\alpha_v\beta_3$

André Raposo Moreira Dias^{+, [a]}, Lizeth Boderó^{+, [b]}, Ana Martins,^[c] Daniela Arosio,^[d] Silvia Gazzola,^[b] Laura Belvisi,^[a, d] Luca Pignataro,^[a] Christian Steinkühler,^[c] Alberto Dal Corso,^[a] Cesare Gennari,^{*, [a, d]} and Umberto Piarulli^{*, [b]}

This work reports the synthesis of a series of small-molecule–drug conjugates containing the $\alpha_v\beta_3$ -integrin ligand *cyclo*[DKP-RGD] or *cyclo*[DKP-*iso*DGR], a lysosomally cleavable Val-Ala (VA) linker or an “uncleavable” version devoid of this sequence, and monomethyl auristatin E (MMAE) or F (MMAF) as the cytotoxic agent. The conjugates were obtained via a straightforward synthetic scheme taking advantage of a copper-catalyzed azide–alkyne cycloaddition as the key step. The conjugates were tested for their binding affinity for the isolated $\alpha_v\beta_3$ receptor and were shown to retain nanomolar IC₅₀ values, in the same range as those of the free ligands. The cytotoxic activity of the

conjugates was evaluated in cell viability assays with $\alpha_v\beta_3$ integrin overexpressing human glioblastoma (U87) and human melanoma (M21) cells. The conjugates possess markedly lower cytotoxic activity than the free drugs, which is consistent with inefficient integrin-mediated internalization. In almost all cases the conjugates featuring *iso*DGR as integrin ligand exhibited higher potency than their RGD counterparts. In particular, the *cyclo*[DKP-*iso*DGR]-VA-MMAE conjugate has low nanomolar IC₅₀ values in cell viability assays with both cancer cell lines tested (U87: 11.50 ± 0.13 nM; M21: 6.94 ± 0.09 nM) and is therefore a promising candidate for in vivo experiments.

Introduction

Monomethyl auristatin E and F (MMAE and MMAF, **1** and **2** in Figure 1) are synthetic analogues of dolastatin 10, a highly cytotoxic pseudopeptide extracted from the sea hare *Dolabella auricularia*. Similar to the original natural product, these analogues exert potent cytotoxic activity by strongly inhibiting microtubule assembly and tubulin-dependent GTP hydrolysis, resulting in cell-cycle arrest and apoptosis.^[1]

Due to their extremely high cytotoxicity, dolastatin analogues cannot be used as drugs themselves and have been exploited as optimal payloads for antibody–drug conjugates (ADCs) and other tumor-targeting strategies.^[2] ADCs have emerged as powerful tools for limiting the main drawbacks of anticancer drugs, such as severe side effects and the emer-

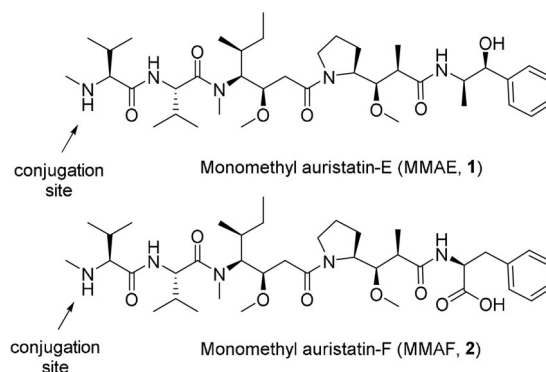


Figure 1. Molecular structures of monomethyl auristatin-E (**1**) and monomethyl auristatin-F (**2**).

gence of multidrug resistance.^[3] Indeed, among the four ADCs approved and commercially available, brentuximab vedotin (AdcetrisTM) bears MMAE linked to an anti-CD30 monoclonal antibody via the protease-cleavable Val-Cit dipeptide linker.^[4] MMAF differs from MMAE in the presence of a charged C-terminal phenylalanine residue, which limits its membrane permeability, attenuating off-target toxicity.^[2a] Although MMAF displays lower cytotoxicity than the more lipophilic MMAE, both drugs have shown similar activity (IC₅₀ values in the subnanomolar range) when released intracellularly by ADCs.^[2a, 5] Moreover, the different physicochemical properties of the two payloads were found to have important implications in the relative mechanism of action in vivo: cell-permeable MMAE is able to diffuse through neighboring cells, extending its toxic activity to other cells in the tumor microenvironment (bystander-killing effect), whereas MMAF is mostly retained inside the



[a] Dr. A. Raposo Moreira Dias,⁺ Prof. Dr. L. Belvisi, Dr. L. Pignataro, Dr. A. Dal Corso, Prof. Dr. C. Gennari
Università degli Studi di Milano, Dipartimento di Chimica, Via C. Golgi, 19, 20133 Milan (Italy)
E-mail: cesare.gennari@unimi.it

[b] Dr. L. Boderó,⁺ Dr. S. Gazzola, Prof. Dr. U. Piarulli
Università degli Studi dell'Insubria, Dipartimento di Scienza e Alta Tecnologia, Via Valleggio, 11, 22100 Como (Italy)
E-mail: umberto.piarulli@uninsubria.it

[c] A. Martins, Dr. C. Steinkühler
Exiris Srl, Via di Castel Romano, 100, 00128 Rome (Italy)

[d] Dr. D. Arosio, Prof. Dr. L. Belvisi, Prof. Dr. C. Gennari
CNR, Istituto di Scienze e Tecnologie Molecolari (ISTM), Via C. Golgi, 19, 20133 Milan (Italy)

[*] These authors contributed equally to this work.

 Supporting information and the ORCID identification number(s) for the author(s) of this article can be found under:
 <https://doi.org/10.1002/cmdc.201900049>

target cancer cell due to its poor membrane permeability, resulting in increased intracellular accumulation.^[6]

In the last decades, low-molecular-weight ligands (e.g., peptides, peptidomimetics, aptamers, vitamins, and substrate analogues) that can be easily accessed by chemical synthesis, have been investigated as carriers for cytotoxic agents, aiming at overcoming important limitations of ADCs, such as high manufacturing costs, unfavorable pharmacokinetics (low tissue diffusion and low accumulation rate), and possible immunogenicity.^[7] Similar to ADCs, the so-called small-molecule–drug conjugates (SMDCs) feature three fundamental parts (i.e., ligand, cytotoxic drug, and linker) and are generally designed to deliver the payload in intracellular compartments of cancer cells (e.g., lysosomes), although non-internalizing SMDCs have also been developed.^[8]

Among the suitable targets for drug delivery, the transmembrane $\alpha_v\beta_3$ integrin receptor is overexpressed on the cell surface of various tumor types (such as melanoma, glioblastoma, renal cell carcinoma, and tumors of lung, ovary, breast, prostate, and colon),^[9] where it is involved in various steps of tumor growth. Since the discovery that endogenous ligands bind integrin $\alpha_v\beta_3$ through the tripeptide sequences Arg-Gly-Asp (RGD)^[10] and *iso*Asp-Gly-Arg (*iso*DGR),^[11] many peptides and peptidomimetics containing these motifs have been designed, leading to high-affinity $\alpha_v\beta_3$ integrin ligands.^[12]

Our research group entered this field by developing cyclic RGD and *iso*DGR integrin ligands containing a bifunctional diketopiperazine (DKP) scaffold.^[13] Notably, the integrin ligands *cyclo*[DKP-RGD] and *cyclo*[DKP-*iso*DGR] (**3** and **4**, Figure 2) displayed low-nanomolar IC_{50} values in competitive binding assays against the purified $\alpha_v\beta_3$ receptor as well as marked selectivity toward the $\alpha_v\beta_3$ receptor relative to $\alpha_v\beta_5$.^[13d]

Later, compounds **3** and **4** were functionalized with a benzylamine moiety (**5** and **6**, Figure 2) allowing their conjugation to different bioactive molecules.^[14–16] Conjugates of the functionalized integrin ligands **5** and **6** with the antimitotic drug paclitaxel (PTX) were synthesized featuring a self-immolative spacer and the lysosomally cleavable Val-Ala (VA) linker.^[15,16] More recently, ligands **5** and **6** were bound to the RNA polymerase II inhibitor α -amanitin via a 6'-ether, giving *cyclo*[DKP-RGD]-VA- α -amanitin and *cyclo*[DKP-*iso*DGR]-VA- α -amanitin conjugates.^[17] Cell viability assays indicated a slightly increased cy-

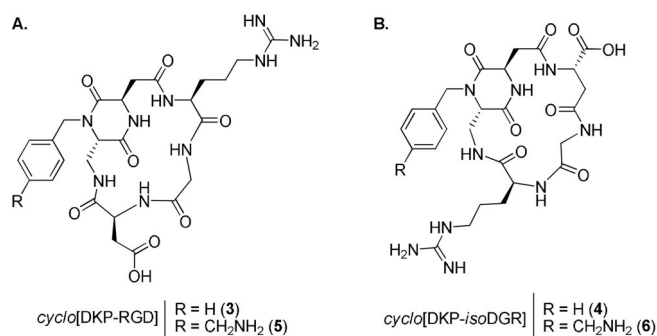


Figure 2. A. ligand *cyclo*[DKP-RGD] (**3**) and its functionalized version (**5**); B. ligand *cyclo*[DKP-*iso*DGR] (**4**) and its functionalized version (**6**).

totoxicity of the *cyclo*[DKP-*iso*DGR]-VA- α -amanitin conjugate relative to the free drug.^[17]

To further investigate the efficacy of our SMDCs, herein we report the synthesis of novel conjugates bearing the $\alpha_v\beta_3$ integrin ligand **5** or **6** and MMAE or MMAF as payload (**7–14**, Figure 3). We evaluated the binding affinity of conjugates **7–14** toward the isolated $\alpha_v\beta_3$ integrin receptor and their cytotoxic activities on human glioblastoma (U87) and human melanoma (M21) cell lines, which are known to overexpress the $\alpha_v\beta_3$ integrin receptor.

Results and Discussion

Synthesis of conjugates 7–14

Conjugates **7–14** (Figure 3), including two *cyclo*[DKP-RGD]-MMAE (**7** and **9**), two *cyclo*[DKP-*iso*DGR]-MMAE (**8** and **10**), two *cyclo*[DKP-RGD]-MMAF (**11** and **13**), and two *cyclo*[DKP-*iso*DGR]-MMAF (**12** and **14**), were synthesized as discussed below. In these conjugates, the integrin ligands are bound to MMAE and MMAF payloads via: 1) a *p*-aminobenzylcarbamate (PABC) self-immolative spacer and a lysosomally cleavable VA linker or an “uncleavable” version devoid of this sequence, 2) a triazole linkage, and 3) a PEG-4 spacer. The synthesis of *cyclo*[DKP-RGD]-MMAE/MMAF (**7**, **9**, **11** and **13**) and *cyclo*[DKP-*iso*DGR]-MMAE/MMAF (**8**, **10**, **12** and **14**) conjugates was performed through the linear synthetic strategy shown in

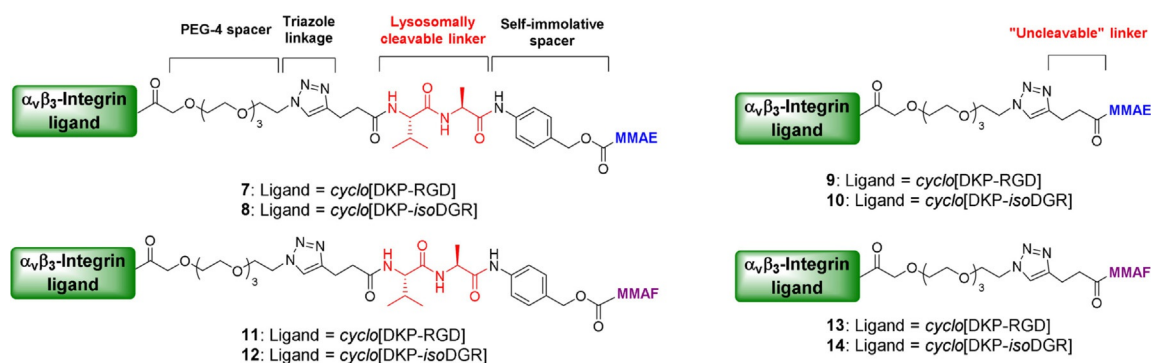
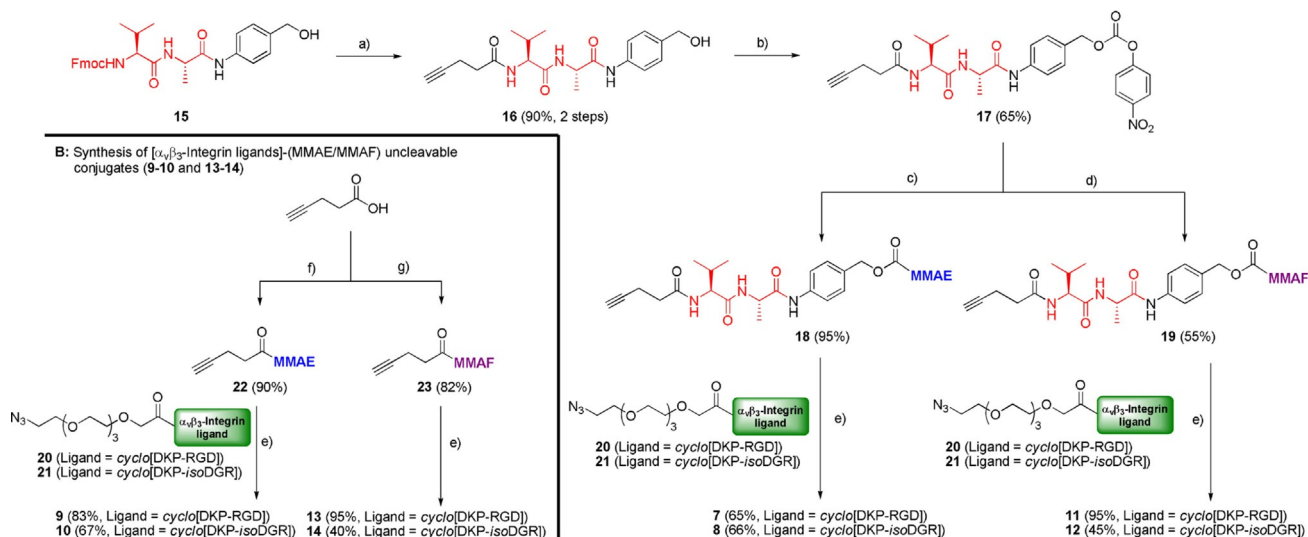


Figure 3. MMAE/MMAF conjugates: *cyclo*[DKP-RGD]-VA-MMAE (**7**), *cyclo*[DKP-*iso*DGR]-VA-MMAE (**8**), *cyclo*[DKP-RGD]-Unc-MMAE (**9**), *cyclo*[DKP-*iso*DGR]-Unc-MMAE (**10**), *cyclo*[DKP-RGD]-VA-MMAF (**11**), *cyclo*[DKP-*iso*DGR]-VA-MMAF (**12**), *cyclo*[DKP-RGD]-Unc-MMAF (**13**), *cyclo*[DKP-*iso*DGR]-Unc-MMAF (**14**).

A: Synthesis of [$\alpha_v\beta_3$ -Integrin ligands]-PEG-4-VA-(MMAE/MMAF) lysosomally cleavable conjugates (7-8 and 11-12)



Scheme 1. Synthesis of conjugates 7–14: a) 1) piperidine, DMF, RT, 2 h; 2) 4-pentynoic acid, HATU, HOAt, *iPr*₂NEt, DMF, RT, overnight; b) 4-nitrophenyl chloroformate, pyridine, RT, THF, 2 h; c) MMAE, HOBT, *iPr*₂NEt, RT, DMF/pyridine (4:1), 65 h; d) MMAF-HCl, HOBT, *iPr*₂NEt, RT, DMF/pyridine (4:1), 65 h; e) ($\alpha_v\beta_3$ -integrin ligand)-PEG-4-N₃, CuSO₄·5 H₂O, NaAsc, DMF/H₂O (1:1), 35 °C, overnight; f) 4-pentynoic acid, MMAE, HATU, HOAt, *iPr*₂NEt, DMF, RT, overnight; g) 4-pentynoic acid, MMAF-HCl, HATU, HOAt, *iPr*₂NEt, DMF, RT, overnight. HATU = 1-[bis(dimethylamino)methylene]-1*H*-1,2,3-triazolo[4,5-*b*]pyridinium 3-oxide hexafluorophosphate; HOAt = 1-hydroxy-7-azabenzotriazole; HOBT = 1-hydroxybenzotriazole; *iPr*₂NEt = *N,N*-diisopropylethylamine; RT = room temperature; NaAsc = sodium ascorbate.

Scheme 1. The Fmoc-protected VA-*p*-aminobenzyl alcohol (15) was synthesized according to a previously reported procedure.^[15] Upon Fmoc removal from 15, the resulting free amine was treated with 4-pentynoic acid, leading to compound 16 in high yield. The latter was then converted into the corresponding 4-nitrophenyl carbonate (17). The secondary amine of MMAE and MMAF was derivatized with the linker by treatment with 4-nitrophenyl carbonate 17, leading to carbamates 18 and 19. The final conjugates 7–8 and 11–12 were obtained through a copper-catalyzed azide–alkyne cycloaddition (CuAAC)^[18] between alkynes 18–19 and the azide-functionalized ligands *cyclo*[DKP-RGD]-PEG-4-N₃ 20^[15] and *cyclo*[DKP-isoDGR]-PEG-4-N₃ 21.^[17]

For the preparation of conjugates bearing an uncleavable linker (9–10 and 13–14, Scheme 1 B), 4-pentynoic acid was reacted with the secondary amine of MMAE and MMAF, affording tertiary amides 22 and 23 in good yields. Then, the CuAAC with functionalized ligands 20 and 21 afforded the uncleavable conjugates 9–10 and 13–14. All final compounds were purified by semipreparative HPLC and lyophilized before biological assays.

$\alpha_v\beta_3$ Integrin receptor competitive binding assays

Conjugates 7–14 were evaluated for their ability to inhibit biotinylated vitronectin binding to the isolated $\alpha_v\beta_3$ receptor. The competitive binding assay was performed by incubating the immobilized integrin receptor with solutions of the *cyclo*[DKP-RGD]-MMAE/MMAF (7, 9, 11, and 13), *cyclo*[DKP-isoDGR]-MMAE/MMAF (8, 10, 12 and 14) conjugates at different concentrations (10⁻¹² to 10⁻⁵ M) in the presence of biotinylated vitronectin (1 μ g mL⁻¹) and measuring bound vitronectin. The

calculated half-maximal inhibitory concentrations (IC₅₀) listed in Table 1 demonstrate that conjugates 7–14 retain good binding affinity for integrin $\alpha_v\beta_3$, with IC₅₀ values in the nanomolar range, similar to or only slightly worse than those of the free ligands 3 and 4.

Table 1. Inhibition of biotinylated vitronectin binding to the isolated $\alpha_v\beta_3$ receptor.

Compound	Structure	IC ₅₀ [nM] ^[a]
3	<i>cyclo</i> [DKP-RGD]	4.5 ± 1.1
4	<i>cyclo</i> [DKP-isoDGR]	9.2 ± 1.1
7	<i>cyclo</i> [DKP-RGD]-VA-MMAE	58.5 ± 10.5
8	<i>cyclo</i> [DKP-isoDGR]-VA-MMAE	36.2 ± 0.2
9	<i>cyclo</i> [DKP-RGD]-Unc-MMAE	40.0 ± 16.1
10	<i>cyclo</i> [DKP-isoDGR]-Unc-MMAE	14.5 ± 0.6
11	<i>cyclo</i> [DKP-RGD]-VA-MMAF	57.8 ± 26.0
12	<i>cyclo</i> [DKP-isoDGR]-VA-MMAF	43.9 ± 2.1
13	<i>cyclo</i> [DKP-RGD]-Unc-MMAF	30.2 ± 12.9
14	<i>cyclo</i> [DKP-isoDGR]-Unc-MMAF	10.7 ± 2.8

[a] IC₅₀ values were calculated as the concentration of compound required for 50% inhibition of biotinylated vitronectin binding to the $\alpha_v\beta_3$ receptor, as estimated by GraphPad Prism software. All values are the arithmetic mean ± SD of duplicate determinations.

Cell viability assays

The antiproliferative activity of compounds 7–14 was evaluated against $\alpha_v\beta_3$ -integrin-overexpressing human glioblastoma (U87) and human melanoma (M21) cells.^[19,20] The cells were treated for 72 hours with increasing doses of free MMAE (1), MMAF (2) and MMAE/MMAF conjugates 7–14, and the cell via-

Table 2. Evaluation of the antiproliferative activity of free MMAE (1) and MMAF (2), and MMAE/MMAF conjugates 7–14 in U87 and M21 cancer cell lines after 72 h incubation.

Compound	IC ₅₀ [nM] ^[a]	
	U87	M21
Free drugs		
MMAE (1)	0.076 ± 0.08	0.065 ± 0.088
MMAF (2)	94.40 ± 0.06	> 1000
Conjugates with <i>cyclo</i>[DKP-RGD]		
<i>cyclo</i> [DKP-RGD]-VA-MMAE (7)	38.99 ± 0.11	55.19 ± 0.06
<i>cyclo</i> [DKP-RGD]-Unc-MMAE (9)	> 1000	320.6 ± 0.10
<i>cyclo</i> [DKP-RGD]-VA-MMAF (11)	385.90 ± 0.09	> 1000
<i>cyclo</i> [DKP-RGD]-Unc-MMAF (13)	> 5000	> 1000
Conjugates with <i>cyclo</i>[DKP-<i>iso</i>DGR]		
<i>cyclo</i> [DKP- <i>iso</i> DGR]-VA-MMAE (8)	11.50 ± 0.13	6.94 ± 0.09
<i>cyclo</i> [DKP- <i>iso</i> DGR]-Unc-MMAE (10)	685.50 ± 0.08	399.8 ± 0.08
<i>cyclo</i> [DKP- <i>iso</i> DGR]-VA-MMAF (12)	165.90 ± 0.05	936.2 ± 0.07
<i>cyclo</i> [DKP- <i>iso</i> DGR]-Unc-MMAF (14)	763.70 ± 0.08	> 1000

[a] IC₅₀ values were calculated as reported in the Supporting Information, from viability curves using GraphPad Prism software. All values are the arithmetic mean ± SD of triplicate determinations.

bility was then evaluated by MTT assay. The calculated IC₅₀ values are listed in Table 2.

Under these experimental conditions, MMAE (1) proved to be much more potent than MMAF (2), confirming published data.^[1,2a] In general, the antiproliferative activity of the integrin-targeted conjugates was found to be lower than the parent free drugs. In the case of the MMAE conjugates with uncleavable linker (9 and 10), the loss of potency is greater than three orders of magnitude ($\geq 5 \times 10^3$). When the linker is cleavable (7 and 8), the potency is still reduced, but to a lesser extent, with the *cyclo*[DKP-*iso*DGR]-VA-MMAE conjugate 8 showing low nanomolar IC₅₀ values, only two orders of magnitude worse than the free drug.

Antibody–MMAF conjugates display IC₅₀ values in the sub-nanomolar range because of assisted internalization. Moreover, antibody–MMAF (and not MMAE) conjugates tolerate uncleavable linkers coupled to the drug N terminus.^[2a,21] These effects are clearly absent in Table 2, where the IC₅₀ values of the integrin ligand–MMAF conjugates are at best in the sub-micromolar range. These results are consistent with the observation that the *cyclo*[DKP-RGD] ligand accumulates on the cell membrane of $\alpha_v\beta_3$ -integrin-expressing cancer cells, while it is poorly internalized by receptor-mediated endocytosis.^[8e]

Finally, our data show that in almost all cases the compounds featuring *cyclo*[DKP-*iso*DGR] as integrin ligand exhibited higher potency than their analogues equipped with *cyclo*[DKP-RGD]. This is evident in comparing *cyclo*[DKP-*iso*DGR]-VA-MMAE (8) and *cyclo*[DKP-RGD]-VA-MMAE (7) both in U87 and M21 cancer cell lines (3.4- and 7.9-fold more potent, respectively).

Conclusions

Conjugation of anticancer drugs to $\alpha_v\beta_3$ integrin ligands represents a promising approach in tumor-targeted chemotherapy. In this work, we synthesized eight conjugates 7–14 bearing

the $\alpha_v\beta_3$ -integrin ligands *cyclo*[DKP-RGD] 3 or *cyclo*[DKP-*iso*DGR] 4 and the potent tubulin polymerization inhibitor MMAE (1) or MMAF (2), widely investigated as payloads in antibody–drug conjugates (ADCs). Conjugates 7, 8 and 11, 12 contain the lysosomally cleavable VA linker, whereas conjugates 9, 10 and 13, 14 present an uncleavable linker. Conjugates 7–14 were found to inhibit biotinylated vitronectin binding to the purified $\alpha_v\beta_3$ receptor at nanomolar concentrations, retaining the excellent integrin binding affinity of the free ligands. In addition, conjugates 7–14 were evaluated in vitro for their activity against the $\alpha_v\beta_3$ -overexpressing U87 and M21 cancer cell lines. Overall, the cell viability data shown in Table 2 indicate that the conjugates bearing both peptidomimetic ligands *cyclo*[DKP-RGD] and *cyclo*[DKP-*iso*DGR] possess lower anticancer activity than the free drugs, which is consistent with inefficient integrin-mediated internalization of the conjugates by the targeted cancer cell.

However, the *iso*DGR-bearing conjugates display a systematically higher anticancer activity than their RGD counterparts, suggesting the possibility that the *cyclo*[DKP-*iso*DGR] is able to promote a more significant internalization with respect to the *cyclo*[DKP-RGD] ligand; this will be explored in future experiments. In particular, the *cyclo*[DKP-*iso*DGR]-VA-MMAE conjugate (8) shows higher activity than *cyclo*[DKP-RGD]-VA-MMAE (7) upon incubation with both U87 and M21 cancer cell lines (3.4- and 7.9-fold, respectively). The low nanomolar IC₅₀ values in both cancer cell lines (U87: 11.50 ± 0.13 nM; M21: 6.94 ± 0.09 nM) suggest that the *cyclo*[DKP-*iso*DGR]-VA-MMAE conjugate (8) is a promising candidate for in vivo experiments, which will be important to obtain evidence of conjugate accumulation at the tumor site. Further studies will include the use of extracellularly cleavable linkers to exploit the passive diffusion properties of MMAE. Indeed, the latter is an emerging strategy in the drug delivery field, supported by recent evidence of promising anticancer activity by non-internalizing ADCs^[22] and SMDCs.^[8e,23]

Experimental Section

MMAE and MMAF drugs are commercially available from Levena Biopharma (USA) and Oskar Tropitzsch GmbH (Germany). Ligands *cyclo*[DKP-RGD] (3) and *cyclo*[DKP-*iso*DGR] (4), their functionalized analogues 5 and 6, Fmoc-Val-Ala-PABA (15) and azide-PEG-4-ligands 20 and 21 were prepared according to the cited literature. The synthetic procedures for the preparation of compounds 7–14 are reported in the Supporting Information, along with the ¹H NMR and ¹³C NMR spectra, HPLC traces, and HRMS spectra. The inhibition assays of biotinylated vitronectin binding to the $\alpha_v\beta_3$ receptor for compounds 7–14 are given in the Supporting Information. The cell antiproliferative studies on U87 and M21 cell lines are also described in the Supporting Information.

Acknowledgements

We thank the European Commission (Marie Skłodowska-Curie ITN MAGICBULLET 642004) for PhD fellowships (to A.R.M.D., L.B., and A.M.) and for financial support. We also gratefully acknowl-

edge Ministero dell'Università e della Ricerca (PRIN 2015 project 20157WW5EH) for financial support.

Conflict of interest

The authors declare no conflict of interest.

Keywords: antitumor agents · auristatins · drug delivery · integrins · peptidomimetics

- [1] a) G. R. Pettit, Y. Kamano, C. L. Herald, A. A. Tuinman, F. E. Boettner, H. Kizu, J. M. Schmidt, L. Baczynski, K. B. Tomer, R. J. Bontems, *J. Am. Chem. Soc.* **1987**, *109*, 6883–6885; b) R. Bai, G. R. Pettit, E. Hamel, *Biochem. Pharmacol.* **1990**, *40*, 1859–1864.
- [2] a) S. O. Doronina, B. A. Mendelsohn, T. D. Bovee, C. G. Cerveny, S. C. Alley, D. L. Meyer, E. Oflazoglu, B. E. Toki, R. J. Sanderson, R. F. Zabinski, A. F. Wahl, P. D. Senter, *Bioconjugate Chem.* **2006**, *17*, 114–124; b) J. A. Francisco, C. G. Cerveny, D. L. Meyer, B. J. Mixan, K. Klussman, D. F. Chace, S. X. Rejniak, K. A. Gordon, R. DeBlanc, B. E. Toki, C.-L. Law, S. O. Doronina, C. B. Siegall, P. D. Senter, A. F. Wahl, *Blood* **2003**, *102*, 1458–1465; c) S. O. Doronina, B. E. Toki, M. Y. Torgov, B. A. Mendelsohn, C. G. Cerveny, D. F. Chace, R. L. DeBlanc, R. P. Gearing, T. D. Bovee, C. B. Siegall, *Nat. Biotechnol.* **2003**, *21*, 778–784; d) S. C. Jeffrey, J. B. Andreyka, S. X. Bernhardt, K. M. Kissler, T. Kline, J. S. Lenox, R. F. Moser, M. T. Nguyen, N. M. Okeley, I. J. Stone, *Bioconjugate Chem.* **2006**, *17*, 831–840; e) S. O. Doronina, T. D. Bovee, D. W. Meyer, J. B. Miyamoto, M. E. Anderson, C. A. Morris-Tilden, P. D. Senter, *Bioconjugate Chem.* **2008**, *19*, 1960–1963; f) M. A. Fanale, *Chellat Oncol.* **2017**, *18*, 1566–1568.
- [3] S. Agnello, M. Brand, M. F. Chellat, S. Gazzola, R. Riedl, *Angew. Chem. Int. Ed.* **2019**, *58*, 3300–3345; *Angew. Chem.* **2019**, *131*, 3336–3383.
- [4] J. Katz, J. E. Janik, A. Younes, *Clin. Cancer Res.* **2011**, *17*, 6428–6436.
- [5] a) M. S. Sutherland, R. J. Sanderson, K. A. Gordon, J. Andreyka, C. G. Cerveny, C. Yu, T. S. Lewis, D. L. Meyer, R. F. Zabinski, S. O. Doronina, P. D. Senter, C. L. Law, A. F. Wahl, *J. Biol. Chem.* **2006**, *281*, 10540–10547; b) Y. Wang, S. Fan, W. Zhong, X. Zhou, S. Li, *Int. J. Mol. Sci.* **2017**, *18*, 1860.
- [6] a) F. Li, K. K. Emmerton, M. Jonas, X. Zhang, J. B. Miyamoto, J. R. Setter, N. D. Nicholas, N. M. Okeley, R. P. Lyon, D. R. Benjamin, C. L. Law, *Cancer Res.* **2016**, *76*, 2710–2719; b) Y. V. Kovtun, V. S. Goldmacher, *Cancer Lett.* **2007**, *255*, 232–240; c) M. Temming, D. L. Meyer, R. Zabinski, P. D. Senter, C. Poelstra, G. Molema, R. J. Kok, *Mol. Pharm.* **2007**, *4*, 686–694.
- [7] S. Cazzamalli, A. Dal Corso, F. Widmayer, D. Neri, *J. Am. Chem. Soc.* **2018**, *140*, 1617–1621.
- [8] a) N. Krall, J. Scheuermann, D. Neri, *Angew. Chem. Int. Ed.* **2013**, *52*, 1384–1402; *Angew. Chem.* **2013**, *125*, 1424–1443; b) G. Casi, D. Neri, *J. Med. Chem.* **2015**, *58*, 8751–8761; c) M. Srinivasarao, C. V. Galliford, P. S. Low, *Nat. Rev. Drug Discovery* **2015**, *14*, 203–219; d) M. Srinivasarao, P. S. Low, *Chem. Rev.* **2017**, *117*, 12133–12164; e) A. Raposo Moreira Dias, A. Pina, A. Dean, H.-G. Lerchen, M. Caruso, F. Gasparri, I. Fraietta, S. Troiani, D. Arosio, L. Belvisi, L. Pignataro, A. Dal Corso, C. Gennari, *Chem. Eur. J.* **2019**, *25*, 1696–1700.
- [9] a) J. S. Desgrosellier, D. A. Cheresh, *Nat. Rev. Cancer* **2010**, *10*, 9–22; b) F. Danhier, A. Le Breton, V. Préat, *Mol. Pharm.* **2012**, *9*, 2961–2973; c) N. De Franceschi, H. Hamidi, J. Alanko, P. Sahgal, J. Ivaska, *J. Cell Sci.* **2015**, *128*, 839–852.
- [10] M. D. Pierschbacher, E. Ruoslahti, *Nature* **1984**, *309*, 30–33.
- [11] Biochemical studies have shown that a spontaneous post-translational modification occurring at the Asn-Gly-Arg (NGR) motif of the extracellular matrix protein fibronectin leads to the isoAsp-Gly-Arg (isoDGR) sequence; see: a) F. Curnis, R. Longhi, L. Crippa, A. Cattaneo, E. Dondossola, A. Bachi, A. Corti, *J. Biol. Chem.* **2006**, *281*, 36466–36476; b) F. Curnis, A. Sacchi, A. Gasparri, R. Longhi, A. Bachi, C. Doglioni, C. Bordignon, C. Traversari, G.-P. Rizzardi, A. Corti, *Cancer Res.* **2008**, *68*, 7073–7082; c) A. Corti, F. Curnis, *J. Cell Sci.* **2011**, *124*, 515–522; d) M. Ghitti, A. Spitaleri, B. Valentini, S. Mari, C. Asperti, C. Traversari, G. P. Rizzardi, G. Musco, *Angew. Chem. Int. Ed.* **2012**, *51*, 7702–7705; *Angew. Chem.* **2012**, *124*, 7822–7825.
- [12] a) K.-E. Gottschalk, H. Kessler, *Angew. Chem. Int. Ed.* **2002**, *41*, 3767–3774; *Angew. Chem.* **2002**, *114*, 3919–3927; b) L. Auzzas, F. Zanardi, L. Battistini, P. Burreddu, P. Carta, G. Rassu, C. Curti, G. Casiraghi, *Curr. Med. Chem.* **2010**, *17*, 1255–1299; c) T. G. Kapp, F. Rechenmacher, S. Neubaer, O. V. Maltsev, E. A. Cavalcanti-Adam, R. Zarka, U. Reuning, J. Notni, H.-J. Wester, C. Mas-Moruno, J. Spatz, B. Geiger, H. Kessler, *Sci. Rep.* **2017**, *7*, 39805.
- [13] a) A. S. M. da Ressurreição, A. Vidu, M. Civera, L. Belvisi, D. Potenza, L. Manzoni, S. Ongeri, C. Gennari, U. Piarulli, *Chem. Eur. J.* **2009**, *15*, 12184–12188; b) M. Marchini, M. Mingozzi, R. Colombo, I. Guzzetti, L. Belvisi, F. Vasile, D. Potenza, U. Piarulli, D. Arosio, C. Gennari, *Chem. Eur. J.* **2012**, *18*, 6195–6207; c) M. Mingozzi, A. Dal Corso, M. Marchini, I. Guzzetti, M. Civera, U. Piarulli, D. Arosio, L. Belvisi, D. Potenza, L. Pignataro, C. Gennari, *Chem. Eur. J.* **2013**, *19*, 3563–3567; d) S. Panzeri, S. Zanella, D. Arosio, L. Vahdati, A. Dal Corso, L. Pignataro, M. Paolillo, S. Schinelli, L. Belvisi, C. Gennari, U. Piarulli, *Chem. Eur. J.* **2015**, *21*, 6265–6271.
- [14] a) R. Colombo, M. Mingozzi, L. Belvisi, D. Arosio, U. Piarulli, N. Carenni, P. Perego, N. Zaffaroni, M. De Cesare, V. Castiglioni, E. Scanziani, C. Gennari, *J. Med. Chem.* **2012**, *55*, 10460–10474; b) M. Mingozzi, L. Manzoni, D. Arosio, A. Da Corso, M. Manzotti, F. Innamorati, L. Pignataro, D. Lecis, D. Delia, P. Seneci, C. Gennari, *Org. Biomol. Chem.* **2014**, *12*, 3288–3302.
- [15] a) A. Dal Corso, M. Caruso, L. Belvisi, D. Arosio, U. Piarulli, C. Albanese, F. Gasparri, A. Marsiglio, F. Sola, S. Troiani, B. Valsasina, L. Pignataro, D. Donati, C. Gennari, *Chem. Eur. J.* **2015**, *21*, 6921–6929; b) S. Zanella, M. Mingozzi, A. Dal Corso, R. Fanelli, D. Arosio, M. Cosentino, L. Schembri, F. Marino, M. De Zotti, F. Formaggio, L. Pignataro, L. Belvisi, U. Piarulli, C. Gennari, *ChemistryOpen* **2015**, *4*, 633–641; c) A. Pina, A. Dal Corso, M. Caruso, L. Belvisi, D. Arosio, S. Zanella, F. Gasparri, C. Albanese, U. Cucchi, I. Fraietta, A. Marsiglio, L. Pignataro, D. Donati, C. Gennari, *ChemistrySelect* **2017**, *2*, 4759–4766; d) A. Raposo Moreira Dias, A. Pina, A. Dal Corso, D. Arosio, L. Belvisi, L. Pignataro, M. Caruso, C. Gennari, *Chem. Eur. J.* **2017**, *23*, 14410–14415; e) P. López Rivas, I. Randelović, A. Raposo Moreira Dias, A. Pina, D. Arosio, J. Tóvári, G. Mező, A. Dal Corso, L. Pignataro, C. Gennari, *Eur. J. Org. Chem.* **2018**, 2902–2909.
- [16] S. Zanella, S. Angerani, A. Pina, P. López Rivas, C. Giannini, S. Panzeri, D. Arosio, M. Caruso, F. Gasparri, I. Fraietta, C. Albanese, A. Marsiglio, L. Pignataro, L. Belvisi, U. Piarulli, C. Gennari, *Chem. Eur. J.* **2017**, *23*, 7910–7914.
- [17] L. Boderó, P. López Rivas, B. Korsak, T. Hechler, A. Pahl, C. Müller, D. Arosio, L. Pignataro, C. Gennari, U. Piarulli, *Beilstein J. Org. Chem.* **2018**, *14*, 407–415.
- [18] a) *1,3-Dipolar Cycloaddition Chemistry*, Wiley, Hoboken (Ed. R. Huisgen), **1984**, Vol. 1, pp. 1–176; b) R. Huisgen, *Pure Appl. Chem.* **1989**, *61*, 613–628; c) H. C. Kolb, M. G. Finn, K. B. Sharpless, *Angew. Chem. Int. Ed.* **2001**, *40*, 2004–2021; *Angew. Chem.* **2001**, *113*, 2056–2075; d) H. C. Kolb, K. B. Sharpless, *Drug Discovery Today* **2003**, *8*, 1128–1137.
- [19] a) S. L. Goodman, H. J. Grote, C. Wilm, *Biol. Open* **2012**, *1*, 329–340; b) N. V. Currier, S. E. Ackerman, J. R. Kintzing, R. Chen, M. F. Interrante, A. Steiner, A. K. Sato, J. R. Cochran, *Mol. Cancer Ther.* **2016**, *15*, 1291–1300.
- [20] E. B. Voura, R. A. Ramjeesingh, A. M. P. Montgomery, C.-H. Siu, *Mol. Biol. Cell.* **2001**, *9*, 2699–2710.
- [21] B. P. Gray, L. Kelly, D. P. Ahrens, A. P. Barry, C. Kratschmer, M. Levy, B. A. Sullenger, *Proc. Natl. Acad. Sci. USA* **2018**, *115*, 4761–4766.
- [22] a) M. Yasunaga, S. Manabe, D. Tarin, Y. Matsumura, *Bioconjugate Chem.* **2011**, *22*, 1776–1783; b) E. Perrino, M. Steiner, N. Krall, G. J. Bernardes, F. Pretto, G. Casi, D. Neri, *Cancer Res.* **2014**, *74*, 2569–2578; c) A. Dal Corso, R. Gébleux, P. Murer, A. Soltermann, D. Neri, *J. Controlled Release* **2017**, *264*, 211–218.
- [23] S. Cazzamalli, B. Ziffels, F. Widmayer, P. Murer, G. Pellegrini, F. Pretto, S. Wulfhart, D. Neri, *Clin. Cancer Res.* **2018**, *24*, 3656–3667.

Manuscript received: January 22, 2019

Revised manuscript received: February 26, 2019

Accepted manuscript online: March 6, 2019

Version of record online: March 22, 2019